

# Weak Decay Process of $B \rightarrow \rho \ell \bar{\nu}_\ell$ :

## A Varying External Field Approach in QCD Sum Rules

Kwei-Chou Yang

*Institute of Physics, Academia Sinica, Taipei, Taiwan 115, R.O.C.*

### Abstract

A varying external field approach in QCD sum rules is formulated in a systematic way to treat the weak decay form factors and their  $q^2$  dependence in the process of  $B \rightarrow \rho \ell \bar{\nu}_\ell$ . From the form factor sum rules, we can also obtain the mass sum rules for  $B$  and  $\rho$  mesons, which can help us determine the reliable Borel windows in studying the relevant form factor sum rules. In this way, we thus demonstrate that some QCD sum rule calculations in the literature are less reliable. We also include induced condensate contributions, which have been ignored, into the relevant sum rules. We obtain the ratios  $\Gamma(\bar{B}^0 \rightarrow \rho^+ e^- \bar{\nu}_e) / \Gamma(\bar{B}^0 \rightarrow \pi^+ e^- \bar{\nu}_e) \approx 0.94$  and  $\Gamma(\bar{B}^0 \rightarrow \rho^+ \tau^- \bar{\nu}_\tau) / \Gamma(\bar{B}^0 \rightarrow \pi^+ \tau^- \bar{\nu}_\tau) \approx 1.15$ . We apply this approach to re-examine the case of the  $D$  meson decay.

PACS number(s): 13.20-v,11.50.Hx,12.38.Lg

## I. INTRODUCTION

Semileptonic decays, because of their simplicity, provide an excellent laboratory where physicists can study the effect of nonperturbative QCD interactions on the weak decay process. A detailed understanding of these processes is also essential for determining the magnitudes of CKM quark-mixing matrix elements.

The weak decay form factors of  $B \rightarrow \rho \ell \bar{\nu}_\ell$  have been calculated by using various approaches. However, the results obtained from the traditional sum rules [1] by considering a three-point correlation function with suitable interpolating current seem to conflict seriously with others' theoretic results, such as light-cone sum rules [2,3], lattice simulations [4], quark models [5–9], and the external field approach of QCD sum rules [10]. Recently, Ball and Braun [11] re-examined such a process by studying the light-cone sum rules with the modified  $\rho$  meson wave functions. In their study, all of the soft (non-perturbative) parts are absorbed into the  $\rho$  meson wave functions. The accuracy of their results is dependent on the shape of the wave functions. Similarly, within the pQCD approach [12], the light meson is described by a phenomenological model function which can be taken, e.g., from QCD sum rules.

In this work, we shall use the varying external field approach of QCD sum rules which has been developed earlier [10] to re-examine the weak decay form factors for  $B \rightarrow \rho \ell \bar{\nu}_\ell$  with a complete calculation. This approach, in spirit, is similar to Ref. [13]. We will present the idea of the induced condensates and show how the induced condensates enter the sum rules. In the calculation we find an additional contribution from the induced condensates, which was ignored in Ref. [10]. Consequently, the  $A_1$  form factor will obtain an additional 10% contribution from the induced condensate, while the other form factors will not. In addition, we also propose a reliable method that can be used to determine the Borel windows in studying the relevant form factor sum rules.

The rest of this paper is organized as follows. The concept of the induced nonlocal condensates will be formulated in the part (a) of Sec. II. In the part (b) of Sec. III, the external field approach of QCD sum rules will be set up to investigate the various decay

form factors of  $B \rightarrow \rho \ell \bar{\nu}_\ell$ . In Sec. IV numerical results and discussion are presented. Sec. V contains a brief summary.

## II. THE METHOD

### A. Quark propagator in the presence of an external variable field

The quark propagator in the external vector (axial vector) field is described by the additional term,  $\Delta\mathcal{L}^{1(2)}$ , in the Lagrangian.

$$\Delta\mathcal{L}^1(x) = -\mathcal{V}^\alpha e^{iqx} J_\alpha^V(x), \quad (1)$$

or

$$\Delta\mathcal{L}^2(x) = -\mathcal{A}^\alpha e^{iqx} J_\alpha^A(x), \quad (2)$$

where

$$J_\alpha^V = \bar{u} \gamma_\alpha b, \quad J_\alpha^A = \bar{u} \gamma_\alpha \gamma_5 b. \quad (3)$$

Here  $\mathcal{V}^\alpha$  ( $\mathcal{A}^\alpha$ ) and  $q^\alpha$  are the amplitude and momentum of the external vector (axial-vector) field, respectively,  $b$  stands for the b quark field operator, and  $u$  is for the u quark field operator. Hence the quark propagator depicted in Fig. 1(a) can be written down as

$$\langle T u_\alpha^b(x) \bar{b}_\beta^a(0) \rangle_{\mathcal{V}(\mathcal{A})} = \langle T u_\alpha^b(x) \bar{b}_\beta^a(0) \rangle_{\mathcal{V}(\mathcal{A})}^{pert} + \langle : u_\alpha^b(x) \bar{b}_\beta^a(0) : \rangle_{\mathcal{V}(\mathcal{A})}^{induced}, \quad (4)$$

with the notation  $\langle \dots \rangle \equiv \langle 0 | \dots | 0 \rangle$ . Here  $a$  and  $b$  are the color indices while  $\alpha$  and  $\beta$  the Lorentz indices. The first term depicted in Fig. 1(b), on the right hand side of Eq. (4), can be calculated from perturbation theory, while the second term depicted in Fig. 1(c) is the induced condensate defined through this paper. Neglecting the radiative corrections, we obtain

$$\langle T u_\alpha^b(x) \bar{b}_\beta^a(0) \rangle_{\mathcal{V}}^{pert} = i \delta^{ab} \int \frac{d^4 p}{(2\pi)^4} e^{-ipx} \frac{[(\not{p} + m_u) \not{\mathcal{V}}((\not{p} + \not{q}) + m_b)]_{\alpha\beta}}{(p^2 - m_u^2)[(p + q)^2 - m_b^2]}. \quad (5)$$

Using the identity [10]:

$$\begin{aligned}
& 12\bar{b}_\beta^a u_\alpha^b \\
&= \left[ 1(\bar{b}u) + \gamma_5(\bar{b}\gamma_5 u) + \gamma^\rho(\bar{b}\gamma_\rho u) - \gamma^\rho\gamma_5(\bar{b}\gamma_\rho\gamma_5 u) + \frac{1}{2}\sigma^{\rho\tau}(\bar{b}\sigma_{\rho\tau} u) \right]_{\alpha\beta} \delta^{ab} \\
&= \left[ 1(\bar{b}u) + \gamma_5(\bar{b}\gamma_5 u) + \gamma^\rho(\bar{b}\gamma_\rho u) - \gamma^\rho\gamma_5(\bar{b}\gamma_\rho\gamma_5 u) + \frac{1}{2}\sigma^{\rho\tau}\gamma_5(\bar{b}\sigma_{\rho\tau}\gamma_5 u) \right]_{\alpha\beta} \delta^{ab}, \tag{6}
\end{aligned}$$

we now project out Eq. (5) on the Dirac matrix basis  $\mathbf{1}$ ,  $\gamma_5$ ,  $\gamma_\rho$ ,  $\gamma_\rho\gamma_5$ ,  $\sigma_{\rho\tau}$ . Thus the induced condensate (the second term on the right hand side of Eq. (4)), with the aid of Eq. (6), is

$$\begin{aligned}
\langle :u_\alpha^b(x)\bar{b}_\beta^a(0): \rangle_{\mathcal{V}}^{induced} &= -\frac{\delta^{ab}}{12} \left( \langle :\bar{b}(0)u(x): \rangle \delta_{\alpha\beta} + \langle :\bar{b}(0)\gamma_5 u(x): \rangle (\gamma_5)_{\alpha\beta} \right. \\
&\quad + \langle :\bar{b}(0)\gamma_\rho u(x): \rangle (\gamma^\rho)_{\alpha\beta} - \langle :\bar{b}(0)\gamma_\rho\gamma_5 u(x): \rangle (\gamma^\rho\gamma_5)_{\alpha\beta} \\
&\quad \left. + \frac{1}{2} \langle :\bar{b}(0)\sigma_{\rho\tau} u(x): \rangle (\sigma^{\rho\tau})_{\alpha\beta} \right)_{\mathcal{V}}^{induced}, \tag{7}
\end{aligned}$$

or

$$\begin{aligned}
\langle :u_\alpha^b(x)\bar{b}_\beta^a(0): \rangle_{\mathcal{A}}^{induced} &= -\frac{\delta^{ab}}{12} \left( \langle :\bar{b}(0)u(x): \rangle \delta_{\alpha\beta} + \langle :\bar{b}(0)\gamma_5 u(x): \rangle (\gamma_5)_{\alpha\beta} \right. \\
&\quad + \langle :\bar{b}(0)\gamma_\rho u(x): \rangle (\gamma^\rho)_{\alpha\beta} - \langle :\bar{b}(0)\gamma_\rho\gamma_5 u(x): \rangle (\gamma^\rho\gamma_5)_{\alpha\beta} \\
&\quad \left. + \frac{1}{2} \langle :\bar{b}(0)\sigma_{\rho\tau}\gamma_5 u(x): \rangle (\sigma^{\rho\tau}\gamma_5)_{\alpha\beta} \right)_{\mathcal{A}}^{induced}, \tag{8}
\end{aligned}$$

where

$$\langle :\bar{b}(0)\Gamma u(x): \rangle_{\mathcal{V}(\mathcal{A})}^{induced} = \langle \text{T}\bar{b}(0)\Gamma u(x) \rangle_{\mathcal{V}(\mathcal{A})} - \langle \text{T}\bar{b}(0)\Gamma u(x) \rangle_{\mathcal{V}(\mathcal{A})}^{pert} \tag{9}$$

with

$$\begin{aligned}
\langle \text{T}\bar{b}(0)\Gamma u(x) \rangle_{\mathcal{V}} &= -i\mathcal{V}^\mu \int d^4z e^{iqz} \langle \text{T}(\bar{u}(z)\gamma_\mu b(z), \bar{b}(0)\Gamma u(x)) \rangle, \\
\langle \text{T}\bar{b}(0)\Gamma u(x) \rangle_{\mathcal{A}} &= -i\mathcal{A}^\mu \int d^4z e^{iqz} \langle \text{T}(\bar{u}(z)\gamma_\mu\gamma_5 b(z), \bar{b}(0)\Gamma u(x)) \rangle, \tag{10}
\end{aligned}$$

and

$$\langle \text{T}\bar{b}(0)\Gamma u(x) \rangle_{\mathcal{V}}^{pert} = -iN_c \int \frac{d^4p}{(2\pi)^4} e^{-ipx} \frac{\text{Tr}[(\not{p} + m_u) \not{\mathcal{V}}(\not{p} + \not{q} + m_b)\Gamma]}{(p^2 - m_u^2)[(p+q)^2 - m_b^2]}, \tag{11}$$

$$\langle \text{T}\bar{b}(0)\Gamma u(x) \rangle_{\mathcal{A}}^{pert} = -iN_c \int \frac{d^4p}{(2\pi)^4} e^{-ipx} \frac{\text{Tr}[(\not{p} + m_u) \not{\mathcal{A}}\gamma_5((\not{p} + \not{q}) + m_b)\Gamma]}{(p^2 - m_u^2)[(p+q)^2 - m_b^2]}. \tag{12}$$

Here  $\Gamma$  is the generic notation for the Dirac matrix basis  $\mathbf{1}$ ,  $\gamma_5$ ,  $\gamma_\rho$ ,  $\gamma_\rho\gamma_5$ ,  $\sigma_{\rho\tau}$  and the path-ordered gauge factor is implied by

$$\mathcal{G}(0, x) = P\exp[-ig_s \int_0^1 d\alpha x^\mu A_\mu(\alpha x)]. \quad (13)$$

In the case of the fixed-point gauge (the Fock-Schwinger gauge)  $x^\mu A_\mu(x) = 0$ , this factor is equal to unity.

## B. The Derivation of QCD Sum Rules

For the form factors of  $B \rightarrow \rho \ell \nu_\ell$ , we consider the following two point Green's function in the external variable vector field  $\mathcal{V}$  or axial-vector field  $\mathcal{A}$ :

$$\Pi_{\mu\nu}^{\mathcal{V}(\mathcal{A})}(p, p'; q^2) = i \int d^4x e^{ip'x} \langle T\{j_\mu(x), j_\nu^5(0)\} \rangle_{\mathcal{V}(\mathcal{A})}, \quad (14)$$

where  $\langle \dots \rangle \equiv \langle 0 | \dots | 0 \rangle$ ,  $j_\mu = \bar{d}\gamma_\mu u$  and  $j_\nu^5 = \bar{b}\gamma_\nu\gamma_5 d$ . The interaction with the external vector field is described by the additional term,  $\Delta\mathcal{L}$ , in the Lagrangian as shown in Eqs. (1) and (2). In the following calculation we consider only the amplitude of  $\Pi_{\mu\nu}^{\mathcal{V}(\mathcal{A})}$  linear in the external field  $\mathcal{V}(\mathcal{A})$ . Generally speaking, the coefficients of tensor structures  $\Pi_i$  in  $T_{\mu\nu}$  can be expressed as a double dispersion relation form:

$$\Pi_i(p, p'; q^2) = \int ds \int ds' \frac{\rho_i(p, p'; q^2)}{(s - p^2)(s' - p'^2)} + \text{subtraction terms}, \quad (15)$$

where the subtraction terms have the form

$$\text{subtraction terms} = P_{1\mu\nu}(p^2) \int \frac{\Delta(s')ds'}{s' - p'^2} + P_{2\mu\nu}(p'^2) \int \frac{\Delta(s)ds}{s - p^2} + P_{3\mu\nu}(p^2, p'^2). \quad (16)$$

One finds that such a contribution from the subtraction terms is of no importance since, after performing the double Borel transform, all of the subtraction terms,  $P_{1\mu\nu}$ ,  $P_{2\mu\nu}$ , and  $P_{3\mu\nu}$ , disappear. (For further discussions, see Ref. [14]) The double Borel transform  $B[\Pi_i]$  on  $\Pi_i$  [10] in both variables  $p^2$  and  $p'^2$  gives

$$B[\Pi_i] = \int_0^\infty ds \int_0^\infty ds' e^{-(s'/M'^2 + s/M^2)} \rho_i \quad (17)$$

The hadronic side of Eq. (14) is represented as a sum over the hadronic states. If the Borel masses are chosen properly, the hadronic side of Eq. (14) will be dominated by the lowest hadronic states with the contributions from the higher states and the continuum suppressed.

At the hadron level (the right hand side), the spectral function of  $\Pi_{\mu\nu}^{A(V)}$  can be written as

$$\begin{aligned}\rho_{\mu\nu}^A &= \mathcal{A}^\alpha \frac{f_B m_\rho^2}{g_\rho} [f g_{\alpha\mu} p_\nu + a_+ p_\mu (p + p')_\alpha p_\nu + a_- p_\mu q_\alpha p_\nu \\ &\quad + \text{other terms...}] \times \delta(s - m_B^2) \delta(s' - m_\rho^2) + \text{higher states,} \\ \rho_{\mu\nu}^V &= \mathcal{V}^\alpha \frac{f_B m_\rho^2}{g_\rho} [2ig \epsilon_{\alpha\mu\beta\rho} p_\nu p'^\beta p^\rho \\ &\quad + \text{other terms...}] \times \delta(s - m_B^2) \delta(s' - m_\rho^2) + \text{higher states,}\end{aligned}\tag{18}$$

where the higher states start from a higher enough value,  $s_0^B$  or  $s_0^\rho$ . The contribution from the higher states could be approximated by the perturbative part, (which starts from the value,  $s_0^B$  or  $s_0^\rho$ ) in the OPE of the quark level. The “other terms” in Eq. (18) are the irrelevant tensor structures that are not taken into account here and thus are suppressed.

Here we have adopted the definitions

$$\begin{aligned}\langle 0 | j_\mu | \rho(p', \lambda) \rangle &= i \frac{m_\rho^2}{g_\rho} \epsilon_{(\lambda)\mu}, \\ \langle \rho(p', \lambda) | J_\alpha^V - J_\alpha^A | B(p) \rangle &= 2ig \epsilon_{\alpha\mu\beta\rho} p'^\mu p^\beta \epsilon_{(\lambda)}^{*\rho} \\ &\quad - f \epsilon_{(\lambda)\alpha}^* - a_+ (\epsilon_{(\lambda)}^* \cdot p) (p + p')_\alpha - a_- (\epsilon_{(\lambda)}^* \cdot p) q_\alpha,\end{aligned}\tag{19}$$

with

$$\begin{aligned}f &= (m_\rho + m_B) A_1, \\ a_+ &= -\frac{A_2}{m_\rho + m_B}, \\ a_- &= 2m_\rho A, \\ A(q^2) &= \frac{A_0(q^2) - A_3(q^2)}{q^2}, \quad A_3(q^2) = \frac{A_1(q^2)(m_\rho + m_B)}{2m_\rho} - \frac{A_2(q^2)(m_B - m_\rho)}{2m_\rho}, \\ g &= \frac{V}{m_\rho + m_B}\end{aligned}$$

in the BSW parametrization [6].

At the quark-gluon level, the Eq. (14) can be alternatively written as

$$\Pi_{\mu\nu}^{\mathcal{V}(\mathcal{A})}(p, p'; q^2) = i \int d^4x e^{ip'x} \langle S_d^{ab}(0, -x) \gamma_\mu \gamma_5 S_{ub}^{ba\mathcal{V}(\mathcal{A})}(x, 0) \gamma_\nu \gamma_5 \rangle, \quad (20)$$

where [10,15]

$$\begin{aligned} S_d^{ab}(0, -x) = & \int \frac{d^4p}{(2\pi)^4} e^{ipx} \left[ \frac{i\delta^{ab}}{\not{p} - m_d} + \frac{i}{4} \frac{\lambda_{ab}^n}{2} g_s G_{\mu\nu}^n(0) \frac{\sigma^{\mu\nu}(\not{p} + m_d) + (\not{p} + m_d)\sigma^{\mu\nu}}{(p^2 - m_d^2)^2} \right. \\ & \left. - \frac{iG_{\mu\nu}^n(0)\lambda_{ab}^n}{4} g_s x^\nu \left( \frac{1}{\not{p} - m_d} \gamma^\mu \frac{1}{\not{p} - m_d} \right) \right] \\ & - \frac{\delta^{ab}}{12} \langle \bar{d}d \rangle + \frac{\delta^{ab}x^2}{192} \langle g_s \bar{d}\sigma G d \rangle \\ & + i g_s^2 \frac{\delta^{ab} \langle \bar{d}d \rangle^2 x^2}{2^5 \times 3^5} \delta^{ab} \not{x} - \frac{i\delta^{ab}}{48} m_d \langle \bar{d}d \rangle \not{x} \end{aligned} \quad (21)$$

and  $S_{ub}^{ba\mathcal{V}(\mathcal{A})}(x, 0) \equiv \langle T u_\alpha^b(x) \bar{b}_\beta^a(0) \rangle_{\mathcal{V}(\mathcal{A})}$  is shown in Eq. (4) but also in the background gluon field. Here we have used the fixed-point gauge,  $x^\mu A_\mu^a(x) = 0$  [15,10] for the gluon field.

The Feynman integral for the bare loop can be written as

$$\begin{aligned} \Pi_{\mu\nu}^{\mathcal{V}}(p, p'; q^2) &= 3i\mathcal{V}^\alpha \int \frac{d^4k}{(2\pi)^4} \frac{\text{Tr}[(\not{p}' + \not{k} + m_u)\gamma_\alpha(\not{k} + m_b)\gamma_\nu\gamma_5(\not{k} + m_d)\gamma_\mu]}{k^2(k + p')^2[(k + p)^2 - m_b^2]}, \\ \Pi_{\mu\nu}^{\mathcal{A}}(p, p'; q^2) &= 3i\mathcal{A}^\alpha \int \frac{d^4k}{(2\pi)^4} \frac{\text{Tr}[(\not{p}' + \not{k} + m_u)\gamma_\alpha\gamma_5(\not{k} + m_b)\gamma_\nu\gamma_5(\not{k} + m_d)\gamma_\mu]}{k^2(k + p')^2[(k + p)^2 - m_b^2]}, \end{aligned} \quad (22)$$

where  $m_u^2$  and  $m_d^2$  have been neglected. The relevant diagram is shown in Fig. 2(a). Using the Cutkosky's rule [16], the integral can be solved easily by taking the imaginary part of the quark propagators:  $1/(p^2 - m_b^2 + i\epsilon) \rightarrow -2\pi i\delta(p^2 - m_b^2)$ . Thus this integral may be recast as a double dispersion relation

$$\Pi_{\mu\nu}^{\mathcal{V}(\mathcal{A})}(p, p'; q^2) = -\frac{\mathcal{V}(\mathcal{A})^\alpha}{4\pi^2} \iint_{\Omega} ds ds' \frac{\rho_{\mu\nu\alpha}^{\mathcal{V}(\mathcal{A})}(s, s'; q^2)}{(s - p^2)(s' - p'^2)}, \quad (23)$$

where

$$\begin{aligned} \rho_{\mu\nu\alpha}^{\mathcal{V}} &= 3i \int \frac{d^4k}{(2\pi)^4} (-2\pi i)^3 \delta(k^2) \delta[(k + p')^2] \delta[(k + p)^2 - m_b^2] \\ & \times \text{Tr}[(\not{p}' + \not{k} + m_u)\gamma_\alpha(\not{k} + m_b)\gamma_\nu\gamma_5(\not{k} + m_d)\gamma_\mu], \\ \rho_{\mu\nu\alpha}^{\mathcal{A}} &= 3i \int \frac{d^4k}{(2\pi)^4} (-2\pi i)^3 \delta(k^2) \delta[(k + p')^2] \delta[(k + p)^2 - m_b^2] \\ & \times \text{Tr}[(\not{p}' + \not{k} + m_u)\gamma_\alpha\gamma_5(\not{k} + m_b)\gamma_\nu\gamma_5(\not{k} + m_d)\gamma_\mu], \end{aligned} \quad (24)$$

and the corresponding integration region  $\Omega$ , which can be solved via the Landau equation, is specified by  $s' > 0$  and  $s > m_b^2 + m_b^2 s' / (m_b^2 - q^2)$ . Note that if  $(m_b^2 - q^2)/q^2 < s'$ , there

may be additional contributions to the above integral because of pinching of the singularities on non-physical sheets [1]. However, at the hadron level, the contribution from the higher states is approximated by the perturbative part, which starts from the thresholds  $s_0^B$  and  $s_0^\rho$ , we therefore study the  $q^2$  behaviors of the form factors in the region:  $0 \leq q^2$  and  $(m_b^2 - q^2)/q^2 > s_0^\rho$ , where  $s_0^\rho$  is the threshold of the excited states,  $s' < s_0^\rho$ . In this region it is not necessary to worry about possible contributions from non-physical sheets. Considering only the leading power corrections of OPE of the correlation function Eq. (4), we obtain [17]

$$\begin{aligned} \Pi_i(p, p'; q^2) = & \int_0^{s_0^B} ds \int_0^{s_0^\rho} ds' \frac{\rho_i^{pert}(p, p'; q^2)}{(s - p^2)(s' - p'^2)} + \Pi_i^{induced} + d_3^i \langle \bar{d}d \rangle + d_5^i \langle g_s \bar{d} \sigma G d \rangle \\ & + d_6^{(1)i} g_s^2 \langle \bar{d}d \rangle^2 + d_6^{(2)i} g_s^2 \langle \bar{d}d \rangle \langle \bar{b}b \rangle + d_6^{(3)i} g_s^2 \langle \bar{d}d \rangle \langle \bar{u}u \rangle + \dots, \end{aligned} \quad (25)$$

where

$$\begin{aligned} \rho_f^{pert} = & \frac{3s'}{4\pi^2 \lambda^{5/2}} \left( 2s'(2s - 2m_b^2 - u)\Delta - \lambda[(m_b^2 - q^2)^2 - s'q^2] \right. \\ & \left. - \lambda m_b(m_u - m_d)(2s' + 2m_b^2 - u) \right), \end{aligned} \quad (26)$$

$$\begin{aligned} \rho_{a_\pm}^{pert} = & \frac{3s'}{4\pi^2 \lambda^{7/2}} \left( 20\Delta s' [\mp u(s \pm s' - m_b^2) - 2s'm_b^2] \right. \\ & \mp \lambda [3\Delta u - 2s'((s - m_b^2)^2 \pm s'(s' + 2m_b^2 - q^2))] \\ & \left. - \lambda^2 (2s' \pm q^2 \mp m_b^2) + C_\pm \right), \end{aligned} \quad (27)$$

$$\rho_g^{pert} = -\frac{3s'}{4\pi^2 \lambda^{5/2}} \left( \lambda(3m_b^2 - 2q^2 - s) + 3\Delta(3s' - s + q^2) \right), \quad (28)$$

with  $u = s + s' - q^2$ ,  $\lambda = u^2 - 4ss'$ ,  $\Delta = (s - m_b^2)(m_b^2 - q^2) - s'm_b^2$ ,  $C_+ = 4s'(20s's\Delta + 6\Delta\lambda - \lambda s's)$ , and  $C_- = 0$ . (See Ref. [10] for the detailed calculation.) Note that in Eq. (25), the contribution from the excited states has been approximately subtracted due to the upper integral limit,  $s_0^B$  or  $s_0^\rho$ , in the first term. To calculate the contribution from the induced condensate,  $\Pi^{induced}$ , we parametrize the bilocal condensate as in Refs. [13,18]:

$$\langle \bar{q}\mathcal{G}(0, x)q(x) \rangle = \langle \bar{q}q \rangle g(x_E^2), \quad (29)$$

with

$$g(x_E^2) = \int_0^\infty f(\alpha) e^{-x_E^2 \alpha/4}, \quad (30)$$

where the coordinates are Euclidean ( $x_E^2 = -x^2$ ) and  $g(x_E^2)$  is the Euclidean space-time correlation function of the vacuum quarks. Our choice of the vacuum function is

$$f(\alpha) = \frac{4}{m_0^2} e^{-4\alpha/m_0^2}, \quad (31)$$

where  $m_0^2 \langle \bar{q}q \rangle = -\langle g_s \bar{q} \sigma^{\mu\nu} G_{\mu\nu} q \rangle$ . The corresponding correlation function  $g(x^2)$  of the vacuum quarks is of the monopole form

$$g(x_E^2) = \frac{1}{1 + m_0^2 x_E^2 / 16}. \quad (32)$$

This choice leads to the empirical sea-quark distribution [18]. By using bilocal condensate parametrized above, we obtain the relevant induced condensate in our study as

$$\langle b(0) \mathcal{G}(0, x) \gamma_\mu \gamma_5 d(x) \rangle_{\mathcal{A}} = \mathcal{A}_\mu \int e^{iqxu} \phi(u) du, \quad (33)$$

with

$$\phi(u) = m_b \langle \bar{d}d \rangle \int_0^\infty \frac{f(\beta)}{\beta} e^{\frac{-m_b^2}{\beta}(\frac{1}{1-u}-1)} e^{q^2 u / \beta} + \mathcal{O}(x^2). \quad (34)$$

Thus we obtain the contribution of the induced condensate, as shown in Fig. 2(b),

$$\Pi_{A_1, \text{Fig.2}(b)}^{induced} = \int_0^1 du \frac{u \phi(u)}{(p' + uq)^2}, \quad (35)$$

and  $\Pi_{A_2, \text{Fig.2}(b)}^{induced} = \Pi_{A, \text{Fig.2}(b)}^{induced} = \Pi_{V, \text{Fig.2}(b)}^{induced} = 0$ . Note that the contribution of the induced condensate in Eq. (35) was ignored in Ref. [10]. The contribution of induced condensates as shown in Fig. 2(c) is given by

$$\begin{aligned} \Pi_{A_1, \text{Fig.2}(c)}^{induced}(p, p'; q^2) &= -\frac{2g_s^2 \langle \bar{d}d \rangle}{9} \chi_{bd}^{\mathcal{A}}(q^2) \frac{p^2 - p'^2 - q^2}{(p^2 - m_b^2)p'^4}, \\ \Pi_{A_2, \text{Fig.2}(c)}^{induced}(p, p'; q^2) &= \frac{2g_s^2 \langle \bar{d}d \rangle}{9} \chi_{bd}^{\mathcal{A}}(q^2) \frac{1}{(p^2 - m_b^2)p'^4}, \\ \Pi_{A, \text{Fig.2}(c)}^{induced}(p, p'; q^2) &= -\frac{2g_s^2 \langle \bar{d}d \rangle}{9} \chi_{bd}^{\mathcal{A}}(q^2) \frac{1}{(p^2 - m_b^2)p'^4}, \\ \Pi_{V, \text{Fig.2}(c)}^{induced}(p, p'; q^2) &= \frac{4g_s^2 \langle \bar{d}d \rangle}{9} \chi_{bd}^{\mathcal{V}}(q^2) \frac{1}{(p^2 - m_b^2)p'^4}, \end{aligned} \quad (36)$$

where the definition of  $\chi^{\mathcal{V}(\mathcal{A})}$  is

$$\begin{aligned}\langle \bar{b}(0)\sigma^{\alpha\beta}u(x)\rangle_{\mathcal{V}} &\approx -i\mathcal{V}^\nu e^{iqx}\chi_{bu}^{\mathcal{V}}(q^2)(g_{\nu\alpha}q_\beta - g_{\beta\nu}q_\alpha), \\ \langle \bar{b}(0)\sigma^{\alpha\beta}\gamma_5 u(x)\rangle_{\mathcal{A}} &\approx -i\mathcal{A}^\nu e^{iqx}\chi_{bu}^{\mathcal{A}}(q^2)(g_{\nu\alpha}q_\beta - g_{\beta\nu}q_\alpha),\end{aligned}\quad (37)$$

and the values of  $\chi^{\mathcal{V}(\mathcal{A})}$  are

$$\chi_{bd}^{\mathcal{V}(\mathcal{A})} = \frac{f^{\mathcal{V}(\mathcal{A})}}{m_{f^{\mathcal{V}(\mathcal{A})}}^2 - q^2} - \frac{3}{8\pi} \int_{m_b^2}^{s_0} ds \frac{m_b}{s - q^2} [1 - 2(\frac{m_Q^2}{s}) + (\frac{m_b^2}{s})^2], \quad (38)$$

where  $f^{\mathcal{V}}=0.28$  GeV<sup>3</sup>,  $f^{\mathcal{A}}=0.67$  GeV<sup>3</sup>,  $s_0^{\mathcal{V}}=33$  GeV<sup>2</sup>, and  $s_0^{\mathcal{A}}=38.2$  GeV<sup>2</sup>. The detailed calculation is shown in Ref. [10]. Note that the uncertainties of our sum rule results are well controlled since in the following numerical analysis we find that the contribution of the induced condensate in Eq. (35) is about 10% to the  $A_1$  sum rule, and that the contribution of Eq. (36) to relevant sum rules is less than 4%. The rest of the results for  $d_i$  is collected in the Appendix. And  $d_3$ ,  $d_5$ ,  $d_6^{(1)}$ ,  $d_6^{(2)}$ , and  $d_6^{(3)}$  are represented pictorially by Figs. 3(d), 3(e), 3(f), 3(g), and 3(h), respectively.

After equating the hadronic side to the quark side and then performing the double Borel transform  $B[f]$  on  $f$  in both variables  $p^2$  and  $p'^2$ , we derive the relevant form factor QCD sum rules as follows:

$$\frac{f_B m_\rho^2}{g_\rho} (m_B + m_\rho) e^{-(m_B^2/M^2)} e^{-(m_\rho^2/M'^2)} A_1(q^2) = B[\Pi_{A_1}^{quark}], \quad (39)$$

$$\frac{f_B m_\rho^2}{g_\rho} \frac{1}{m_B + m_\rho} e^{-(m_B^2/M^2)} e^{-(m_\rho^2/M'^2)} A_2(q^2) = -B[\Pi_{A_2}^{quark}], \quad (40)$$

$$\frac{f_B m_\rho^2}{g_\rho} 2m_\rho^2 e^{-(m_B^2/M^2)} e^{-(m_\rho^2/M'^2)} A(q^2) = B[\Pi_A^{quark}], \quad (41)$$

$$\frac{f_B m_\rho^2}{g_\rho} \frac{2}{m_B + m_\rho} e^{-(m_B^2/M^2)} e^{-(m_\rho^2/M'^2)} V(q^2) = B[\Pi_V^{quark}]. \quad (42)$$

### III. RESULTS AND DISCUSSION

#### A. The determination of Borel windows

In numerical analyses of form factors, people usually assume, according to the empirical observation [19], that the suitable region of sum rules is at values of Borel masses twice as

large as that in the corresponding two-point functions [1,20] and thus extract results from larger Borel mass regions. However, we will provide a detailed analysis to show that such choice is not always correct.

To obtain reliable Borel windows in which the form factor sum rules may be safely used in the analysis, we apply the differential operator  $-M'^4 \partial \ln/\partial M'^2$  to both sides of Eq. (39) and then obtain the  $\rho$  mass sum rule, which is free of the parameters  $g_\rho$ ,  $f_B$ , and the form factors ( $A_1$ ,  $A_2$ ,  $A$ , or  $V$ ). This procedure is usually used in analyzing the mass sum rules in the two-point Green's function approach [21,15]. Analogously, we also obtain the  $\rho$  meson mass rules from Eqs. (40), (41), and (42). On the other hand, when applying the differential operator  $-M^4 \partial \ln/\partial M^2$  to both sides of Eqs. (39-42), we obtain four  $B$  meson mass sum rules. Totally, we obtain eight mass rules (four for the  $\rho$  meson and four for the  $B$  meson). In the numerical analysis, we use the the following set of parameters:

$$m_b = 4.7 \text{ GeV}, \quad m_u = m_d = 0, \quad \langle \bar{u}u \rangle = \langle \bar{d}d \rangle = -(240 \text{ MeV})^3, \quad m_0^2 = 0.6 - 0.8 \text{ GeV}^2, \quad (43)$$

where  $m_b$  is a pole mass. The heavy quark condensate will be dismissed through this paper. To further improve the validity of the derived QCD sum rules, we have performed the following replacements:

$$m_s \rightarrow m_s L^{-\frac{4}{b}}, \quad m_0^2 \langle \bar{q}q \rangle \rightarrow m_0^2 \langle \bar{q}q \rangle L^{-\frac{2}{3b}}, \quad \langle \bar{q}q \rangle \rightarrow \langle \bar{q}q \rangle L^{\frac{4}{b}}, \quad (44)$$

with

$$L = \frac{\ln((M'^2 M^2)^{1/2}/\Lambda^2)}{\ln(\mu^2/\Lambda^2)}, \quad (45)$$

$\Lambda=100$  MeV,  $\mu=500$  MeV, and  $b = 11 - 2n_f/3$  with  $n_f$  being the number of *unfrozen* quark flavors. Note also that region  $R^{-1} \ll Q^2 \ll m_b^2$ , where  $R$  is the confinement radius, exists an anomalous dimension  $2/b$  for both of the current operators [22–24],  $\bar{b}\gamma_\nu\gamma_5 q$  and  $\bar{b}\gamma_\nu q$ . In our numerical analysis of  $B$  meson decay form factors, the sum rules are studied at  $Q^2 \sim \sqrt{M'^2 M^2} \approx 3.4 \text{ GeV}^2$  [see below, Eq.(47)]. Therefore, to obtain physical form factors, which

are independent of the subtraction scale, we put the factor  $[\ell n(m_b^2/\Lambda^2)/\ell n((M'^2 M^2)^{\frac{1}{2}}/\Lambda^2)]^{\frac{12}{25}}$  in the relevant form factor sum rules (the right hand side of Eqs. (39-42)). The requirement of obtaining reasonable mass results from these eight mass sum rules puts severe constraints on the choices of the parameters,  $s_0^B$  and  $s_0^\rho$ . With a careful study, we find that the best choice of parameters in our analysis is

$$s_0^B = 33 - 35 \text{ GeV}^2, \quad s_0^\rho = 1.3 - 1.4 \text{ GeV}^2. \quad (46)$$

Consequently we find that

$$8.5 \text{ GeV}^2 < M^2 < 11.5 \text{ GeV}^2, \quad 0.9 \text{ GeV}^2 < M'^2 < 1.2 \text{ GeV}^2 \quad (47)$$

are the reasonable choices through this paper. The resultant masses are  $m_\rho = 0.787 \pm 0.065$  GeV and  $m_B = 5.11 \pm 0.18$  GeV. The detailed results are collected in Table I. As examples in Fig. 3(a) and Fig. 3(b), we plot the  $\rho$  mass and  $B$  mass (extracted from Eq.(39)), respectively, as a function of  $M^2$  and  $M'^2$ . Obviously, the study of both of the  $\rho$  and  $B$  mass sum rules is a gauge to understand the reliability of performing further numerical analyses on the form factors. In concluding this subsection, we will discuss two “traditional” sum rule calculations by considering a three-point correlation function in the existing literature:

The first is the work in Ref. [1] in which the authors use the vector current  $\bar{d}\gamma^\nu u$  and the pseudoscalar current  $\bar{b}\gamma_5 d$  as the interpolating fields for the  $\rho$  meson and for the  $B$  meson, respectively. For the form factor  $A_1$ , they obtain the following sum rule:

$$\begin{aligned} A_1 & \frac{f_B(m_B + m_\rho)m_B^2 m_\rho^2}{m_b g_\rho} e^{-(m_B^2/M^2)} e^{-(m_\rho^2/M'^2)} \\ &= \frac{3}{4\pi^2} \int_0^{s_0^B} ds \int_0^{s_0^\rho} ds' e^{-(s/M^2)} e^{-(s'/M'^2)} \left( \frac{m_b s' + m_u(s - m_b^2)}{2\lambda^{1/2}} \right. \\ & \quad \left. + \frac{m_b s' [(s - m_b^2)(q^2 - m_b^2) + s' m_b^2]}{\lambda^{3/2}} \right) \\ & \quad - \langle \bar{q}q \rangle \left( m_b m_u + \frac{m^2 - q^2}{2} \right) e^{-m_b^2/M^2} \\ & \quad + \langle \bar{q}q \rangle m_0^2 \left( \frac{-1}{6} + \frac{(2m_b^2 + 3m_b m_u - 2q^2)(m_b^2 - q^2)}{12M^2 M'^2} \right. \\ & \quad \left. - \frac{2m_b^2 + 3m_b m_u - 2q^2}{12M'^2} - \frac{3m_b^2 + 9m_b m_u - 4q^2}{12M^2} + m_b^2 \frac{m_b^2 + 2m_b m_u - q^2}{8M^4} \right) e^{-m_b^2/M^2} \end{aligned}$$

$$\begin{aligned}
& + \frac{16\alpha_s\pi\langle\bar{q}q\rangle^2 m_b}{9} \left( \frac{8}{9M'^2} - \frac{1}{9M^2} + \frac{1}{(m_b^2 - q^2)} + \frac{3m_b^2 - 2q^2}{72M^4} - \frac{m_b^2 - q^2}{6M^2M'^2} \right. \\
& \quad \left. + \frac{m_b^2(m_b^2 - q^2)}{72M^6} + \frac{(m_b^2 - q^2)^2}{36M^4M'^2} \right) e^{-m_b^2/M^2}, \tag{48}
\end{aligned}$$

where  $\lambda$  is defined as before. From their  $A_1$  sum rule, one can extract, following the procedure shown as above, the  $\rho$  meson mass sum rule. The result is illustrated in Fig. 4(a), from which we see that their result of  $\rho$  mass sum rule is not so stable as to determine the suitable Borel windows. Moreover, one can easily find that once a Borel window is determined, the resultant  $\rho$  mass from their  $A_2$  or  $V$  sum rule is twice as large as that from the  $A_1$  sum rule. Note that if we adopt the varying external field to do the calculation again, we find that various induced condensates may enter complicatedly the sum rules for  $A_1$ ,  $A_2$ , and  $V$  and the contribution from induced condensates becomes a little big. Thus the estimate of the sum rule is less reliable.

The second calculation is done by Ball and Braun [11]. They use the tensor current  $\bar{d}\sigma^{\nu\sigma}u$  and the pseudoscalar current  $\bar{b}\gamma_5d$  as the interpolating fields for the  $\rho$  meson and for the  $B$  meson, respectively. For the form factor  $A_2$ , they have

$$\begin{aligned}
A_2 & \frac{f_B f_\rho^\perp m_B^2}{m_b(m_B + m_\rho)} e^{-(m_B^2/M^2)} e^{-(m_\rho^2/M'^2)} \\
& = \frac{3}{4\pi^2} \int_0^{s^B} ds \int_0^{s^0} ds' e^{-(s/M^2)} e^{-(s'/M'^2)} \left( \frac{(s - m_b^2)u - 2ss'}{\lambda^{3/2}} \right. \\
& \quad \left. - \frac{(s - m_b^2)(s - m_b^2 + 2s')u^2 - 3s'[(s - m_b^2)^2 + 2(s - m_b^2)s + ss']u}{\lambda^{5/2}} \right. \\
& \quad \left. - \frac{2ss'[(s - m_b^2)^2 + 2(s - m_b^2)s' + 3ss']}{\lambda^{5/2}} \right) \\
& - \frac{m_b m_0^2 \langle\bar{q}q\rangle}{6M^2M'^2} e^{-m_b^2/M^2} \\
& - \frac{16\alpha_s\pi\langle\bar{q}q\rangle^2}{9} \left( \frac{1}{6M'^4} + \frac{1}{3M^2M'^2} + \frac{m_b^2}{36M^4M'^2} - \frac{m_b^2 - q^2}{18M^2M'^4} \right) e^{-m_b^2/M^2}, \tag{49}
\end{aligned}$$

where  $u$  and  $\lambda$  are defined as before. Note that, for this  $A_2$  sum rules, one obtains the same result if adopting the varying external field approach. In Fig. 4(b) we show the  $\rho$  mass sum rule extracted from Eq. (49). From Fig. 4(b) we obtain  $m_\rho^2 \leq 0$ . The result seems to indicate that the tensor current  $\bar{d}\sigma^{\nu\sigma}u$  is not a good interpolating field for the  $\rho$  meson as mentioned in Ref. [25]. In the same reference, the authors have pointed out that the tensor

current cannot easily produce a stable  $\rho$  mass sum rule if the vacuum saturation hypothesis goes in the opposite direction:

$$\langle \bar{q}\gamma_5\lambda^a q \bar{q}\gamma_5\lambda^a q \rangle = -\frac{4}{9}(1 + \beta_5)\langle \bar{q}q \rangle^2, \quad (50)$$

with  $\beta_5 \approx -2$ . Moreover, the authors [25] have also shown that the threshold of the excited states in their  $\rho$  meson mass sum rule turns out to be unphysically low, the sum rule is dominated by the continuum contribution, and the power corrections are rather large.

## B. Numerical analysis of form factors

To study numerically the form factors, we adopt the set of parameters as shown in Eqs. (40), (43), and [10]

$$f_B = 160 \text{ MeV}, \quad g_\rho = 3.84. \quad (51)$$

The working Borel windows, which have been determined previously (Eq. (47)), are  $8.5 \text{ GeV}^2 < M^2 < 11.5 \text{ GeV}^2$  and  $0.9 \text{ GeV}^2 < M'^2 < 1.2 \text{ GeV}^2$ . In these Borel ranges, the form factors are dominated by the leading perturbative bare loop; for the  $A_1$  form factor, the absolute value of the contribution of  $\langle g_s \bar{d}\sigma G d \rangle$  is less than 50% of the bare loop. Moreover, the contribution of induced condensate amounts to about 14% to the  $A_1$  sum rule, while less than 4% to  $A_2$ ,  $A$ , or  $V$ . Note that unlike light-cone sum rules [3,11], we cannot apply “directly” the heavy quark limit,  $m_b \rightarrow \infty$ , to these sum rules since in that limit the series of the operator product expansion (OPE) may become unconvengent. But in the case of the  $B$  or  $D$  meson, our results indicate that the series of the OPE is in good convergence. In Fig. 3(a-d), we plot the  $A_1$ ,  $A_2$ ,  $A$ , and  $V$  form factors at  $q^2 = 0$ , respectively, as a function of  $M^2$  and  $M'^2$ . We thus obtain the results on the form factors at  $q^2 = 0$ :

$$\begin{aligned} A_1(0) &= 0.12 \pm 0.01, \\ A_2(0) &= 0.12 \pm 0.01, \\ A(0) &= 0.015 \pm 0.02, \\ V(0) &= 0.15 \pm 0.02, \end{aligned} \quad (52)$$

where the error comes from the variation in the Borel mass,  $s_0^B$ ,  $s_0^\rho$ , or  $m_0^2$ . The resultant values of form factors are half as large as the light-cone sum rule results [3,11] or lattice QCD calculation [4]. We now consider the  $q^2$  dependence of the various form factors. The variation of the form factors with  $q^2$  is of great interest, since it probes the effects of strong interactions on the decay. As the property of discontinuity in Ref. [1] is mentioned (see also the discussion below Eq. (24)), the sum rules work well in the region  $(m_Q^2 - q^2)^2/q^2 > s'_0$ . Therefore, we could obtain the  $q^2$  dependence of the form factors over a wide range of  $q^2$  (from  $q^2=0$  up about to 9 GeV $^2$ ). The  $q^2$  dependence of our form factors is given by

$$F(q^2) = F(0)(1 - q^2/m_F^2)^{-n}, \quad (53)$$

where  $n = 1$  for  $A_1$ ,  $n = 2$  for  $A_2$ ,  $A$ , and  $V$ , and the fitted pole masses are  $m_{A_1}=5.45$  GeV,  $m_{A_2}=6.14$  GeV,  $m_A=5.98$  GeV and  $m_V=5.78$  GeV, respectively. Here the results are evaluated at the central values of the Borel mass ranges in Eq.(47). We find that our  $q^2$  dependence of the form factors is well consistent with the pole model ansatz by Körner and Schuler [5] and recent lattice results [4] as well. In the following calculation, we will extrapolate our  $q^2$  dependence of form factors to all possible kinematic region. The pole model ansatz may be a good approximation for the form factor behavior since it is consistent with this sum rule calculation in the region:  $0 \text{ GeV}^2 < q^2 < 9 \text{ GeV}^2$  and also in good accordance with the QCD power counting rules [26] at large  $-q^2$  (the hard rescattering region). Moreover, by neglecting the light meson mass, we roughly obtain from Eq. (53) the relation  $F(q_m^2)/F(0) \sim m_b^n$ , where  $q_m^2 = (m_b - m_\rho)^2$ . Therefore, our results agree with the prediction of heavy quark symmetry [27] in the kinematic region near zero recoil ( $q^2 \approx q_m^2$ ),

$$\begin{aligned} a_+ + a_- &\sim m_M^{-3/2}, & -a_+ + a_- &\sim m_M^{-1/2}, \\ g &\sim m_M^{-1/2}, & f &\sim m_M^{1/2}. \end{aligned} \quad (54)$$

In Fig. 6(a) we plot the lepton-pair invariant mass spectrum  $d\Gamma/dq^2$  of the  $B \rightarrow \rho \ell \bar{\nu}_\ell$  decay together with  $d\Gamma_L/dq^2$ ,  $d\Gamma_+/dq^2$ , and  $d\Gamma_-/dq^2$ . The solid curve is for  $d\Gamma/dq^2$ , and the long-dashed curve is for  $d\Gamma_L/dq^2$ , the portion of the rate with a longitudinal polarized  $\rho$  in

the final state, the short-dashed curve is for  $d\Gamma_-/dq^2$ , the portion of the rate with a helicity minus  $\rho$  in the final state, while the dotted curve is for  $d\Gamma_+/dq^2$ , the portion of the rate with a helicity positive  $\rho$  in the final state. Similarly, in Fig. 6(b) we plot the electron spectrum  $d\Gamma/dE_e$  of the  $B \rightarrow \rho \ell \bar{\nu}_\ell$  together with  $d\Gamma_L/dE_e$ ,  $d\Gamma_+/dE_e$ , and  $d\Gamma_-/dE_e$ . The solid curve is for  $d\Gamma/dE_e$ , the long-dashed curve for  $d\Gamma_L/dE_e$ , the short-dashed curve for  $d\Gamma_-/dE_e$ , and the dotted curve for  $d\Gamma_+/dE_e$ . Both of the Figs. 6(a) and 6(b) are plotted in the  $B$  meson rest frame.

From Fig. 6 we obtain  $d\Gamma/dq^2 \approx d\Gamma_L/dq^2$  and  $d\Gamma/dE_e \approx d\Gamma_L/dE_e$  at the maximum recoil region ( $q^2 \approx 0$ ). This is quite reasonable because at low  $q^2$ , the electron and antineutrino are nearly collinear, so that their net spin along their motion is zero. Since the  $B$  meson has spin zero, the energetic recoiling  $\rho$  meson must also have zero helicity. The helicity minus contribution is more weighted towards the large  $q^2$  value than the helicity zero contribution around the small  $q^2$  region. Our results also show that  $d\Gamma_-/dq^2 \gg d\Gamma_+/dq^2$  as expected from the left-chiral  $b_L \rightarrow u_L$  transition. Our results for the decay rate are given by

$$\begin{aligned} \Gamma(\bar{B}^0 \rightarrow \rho^+ \ell^- \bar{\nu}_\ell) &= (5.1 \pm 1.0) \times |V_{ub}|^2 \times 10^{12} s^{-1}, \\ \Gamma_L/\Gamma_T &= 0.85 \pm 0.03, \quad \Gamma_+/\Gamma_- = 0.077 \pm 0.012, \\ \Gamma(\bar{B}^0 \rightarrow \rho^+ \tau^- \bar{\nu}_\tau) &= (3.1 \pm 0.06) \times |V_{ub}|^2 \times 10^{12} s^{-1}. \end{aligned} \quad (55)$$

Since the induced condensate like Eq. (35) does not contribute to the sum rules in Ref. [10] for  $\bar{B}^0 \rightarrow \pi^+ \ell^- \bar{\nu}_\ell$ , therefore we take  $\Gamma(\bar{B}^0 \rightarrow \pi^+ e^- \bar{\nu}_e) = (5.4 \pm 1.6) \times |V_{ub}|^2 \times 10^{12} s^{-1}$  and  $\Gamma(\bar{B}^0 \rightarrow \pi^+ \tau^- \bar{\nu}_\tau) = (2.7 \pm 0.07) \times |V_{ub}|^2 \times 10^{12} s^{-1}$  from Ref. [10]. We obtain the ratios  $\Gamma(\bar{B}^0 \rightarrow \rho^+ e^- \bar{\nu}_e) / \Gamma(\bar{B}^0 \rightarrow \pi^+ e^- \bar{\nu}_e) \approx 0.94$  and  $\Gamma(\bar{B}^0 \rightarrow \rho^+ \tau^- \bar{\nu}_\tau) / \Gamma(\bar{B}^0 \rightarrow \pi^+ \tau^- \bar{\nu}_\tau) \approx 1.15$ . Our result for the decay rate  $\Gamma(\bar{B}^0 \rightarrow \pi^+ e^- \bar{\nu}_e)$  is a bit smaller than, but still consistent with the CLEO experimental value [28,29] of  $1.4 \pm 0.6$ . However, one should note that in the CLEO experiment, the reconstruction of the relevant events is model dependent. For instance, if the ISGW II model is used, the ratio  $\Gamma(\bar{B}^0 \rightarrow \rho^+ e^- \bar{\nu}_e) / \Gamma(\bar{B}^0 \rightarrow \pi^+ e^- \bar{\nu}_e)$  is  $1.1 \pm 0.7$ .

In closing this subsection, we consider the case of the D meson decays. By following the

same procedure as the case of  $\bar{B}^0 \rightarrow \rho^+ \ell^- \bar{\nu}_\ell$ , and using the parameters as in Ref. [10], we can obtain the same form factor results and their  $q^2$  behaviors as in Ref. [10], except that  $A_1^{D \rightarrow \rho}(0)$  becomes  $0.43 \pm 0.04$  and  $A_1^{D \rightarrow K^*}(0)$  becomes  $0.61 \pm 0.04$ . The results for the form factors at  $q^2 = 0$  are collected in Table II. The calculated decay rates read

$$\begin{aligned} \Gamma(D^0 \rightarrow \rho^- \ell^+ \nu_\ell) &= 0.44 \pm 0.08 |V_{cd}|^2 \times 10^{11} s^{-1}, \\ \Gamma_L/\Gamma_T &= 0.58 \pm 0.05, \quad \Gamma_+/\Gamma_- = 0.041 \pm 0.002, \\ \Gamma(D^+ \rightarrow K^{*0} \ell^+ \nu_\ell) &= 0.51 \pm 0.06 |V_{cs}|^2 \times 10^{11} s^{-1}, \\ \Gamma_L/\Gamma_T &= 0.99 \pm 0.06, \quad \Gamma_+/\Gamma_- = 0.19 \pm 0.02. \end{aligned} \quad (56)$$

Taking  $|V_{cs}| = 0.975$ , we obtain  $B(D^+ \rightarrow K^{*0} \ell^+ \nu_\ell) = 5.1 \pm 0.7 \%$ . The experimental results [30] are  $B(D^0 \rightarrow K^{*-} \ell^+ \nu_\ell) = 4.8 \pm 0.4 \%$ ,  $\Gamma_L/\Gamma_T = 1.23 \pm 0.13$ ,  $\Gamma_+/\Gamma_- = 0.16 \pm 0.04$ . Our results are consistent with the existing experimental data, except that the value of  $\Gamma_L/\Gamma_T$  is a little smaller than the experimental data. Further applications of this approach to various exclusive decay processes will be published elsewhere [31].

#### IV. SUMMARY

In summary, we have used the varying external field approach of QCD sum rules to compute the form factors for the semileptonic decays  $\bar{B}^0 \rightarrow \rho^+ \ell^- \bar{\nu}_\ell$ . We have formulated this approach in a systematic way. By extracting both of the  $B$  meson and  $\rho$  meson mass sum rules, we can thus determine the reliable Borel windows in studying the relevant form factor sum rules. We also include induced condensate contributions, which have been ignored before, into the relevant sum rules. Therefore, we demonstrate that some QCD sum rule calculations in the literature are less reliable. Our results strongly support the pole model ansatz by Körner and Schuler on the  $q^2$  dependence of the form factors. Combining with the previous analysis in Ref. [10], we obtain the ratio  $\Gamma(\bar{B}^0 \rightarrow \rho^+ e^- \bar{\nu}_e)/\Gamma(\bar{B}^0 \rightarrow \pi^+ e^- \bar{\nu}_e) \approx 0.94$  and  $\Gamma(\bar{B}^0 \rightarrow \rho^+ \tau^- \bar{\nu}_\tau)/\Gamma(\bar{B}^0 \rightarrow \pi^+ \tau^- \bar{\nu}_\tau) \approx 1.15$ .

## ACKNOWLEDGMENTS

The author would like to thank Prof. H.-Y. Cheng and Prof. Hoi-Lai Yu for useful discussions and Prof. H.-Y. Cheng for a careful reading of the manuscript. This work was supported in part by the National Science Council of R.O.C. under Contract No. NSC86-2112-M01-020.

## APPENDIX A:

The quantities  $d_3$ ,  $d_5$ ,  $d_6^{(1)}$ ,  $d_6^{(2)}$ , and  $d_6^{(3)}$  defined in Eq. (25) read

$$d_3^{A_1} = -\frac{m_u}{p'^2(p^2 - m_b^2)} + \frac{m_d}{2(p^2 - m_b^2)^2} + \frac{m_d(m_b^2 - q^2)}{2p'^2(p^2 - m_b^2)^2}, \quad (A1)$$

$$\begin{aligned} d_5^{A_1} = & \frac{1}{12} \left[ -\frac{6m_d m_b^2}{(p^2 - m_b^2)^4} - \frac{2m_d}{(p^2 - m_b^2)^3} + \frac{4m_b - 2m_u + 3m_d}{p'^2(p^2 - m_b^2)^2} - \frac{2m_u + m_d}{p'^4(p^2 - m_b^2)} \right. \\ & + \frac{2(2m_d - m_u)(m_b^2 - q^2)}{p'^4(p^2 - m_b^2)^2} - \frac{4(2m_b^2 - q^2)m_d + 6m_u m_b^2}{p'^2(p^2 - m_b^2)^3} + \frac{2m_d(m_b^2 - q^2)^2}{p'^4(p^2 - m_b^2)^3} \\ & \left. - \frac{6m_d m_b^2(m_b^2 - q^2)}{p'^2(p^2 - m_b^2)^4} \right], \end{aligned} \quad (A2)$$

$$\begin{aligned} d_6^{(1)A_1} = & +\frac{1}{81} \left[ \frac{3}{p'^4(p^2 - m_b^2)} + \frac{2}{p'^2(p^2 - m_b^2)^2} - \frac{2}{(p^2 - m_b^2)^3} \right. \\ & - \frac{10m_b^2 + 28m_b m_u - 2q^2}{p'^2(p^2 - m_b^2)^3} + \frac{6(m_b^2 - q^2) + 7m_b m_u}{p'^4(p^2 - m_b^2)^2} + \frac{6m_b^2}{(p^2 - m_b^2)^4} \\ & \left. + \frac{2(m_b^2 - q^2)(m_b^2 + m_b m_u - q^2)}{p'^4(p^2 - m_b^2)^3} + \frac{6m_b^2(m_b^2 + m_b m_u - q^2)}{p'^2(p^2 - m_b^2)^4} \right], \end{aligned} \quad (A3)$$

$$\begin{aligned} d_6^{(2)A_1} = & \frac{2}{9} \left[ \frac{1}{p^4(p^2 - m_b^2)} + \frac{1}{p'^4 p^2} \right. \\ & \left. + \frac{2m_u m_b^2 + m_b^2 - q^2}{p^4(p^2 - m_b^2)p'^2} - \frac{4m_u m_b^2}{p^2(p^2 - m_b^2)^2 p'^2} \right], \end{aligned} \quad (A4)$$

$$d_6^{(3)A_1} = -\frac{4}{9} \frac{1}{p'^4(p^2 - m_b^2)}, \quad (A5)$$

$$d_3^{A_2} = 0, \quad (A6)$$

$$d_5^{A_2} = -\frac{m_u}{6p'^4(p^2 - m_b^2)^2} - \frac{m_d}{6p'^2(p^2 - m_b^2)^3}, \quad (\text{A7})$$

$$d_6^{(1)A_2} = -\frac{1}{27} \left[ \frac{2}{p'^2(p^2 - m_b^2)^3} + \frac{1}{p'^4(p^2 - m_b^2)^2} \right], \quad (\text{A8})$$

$$d_6^{(2)A_2} = -\frac{2}{9m_b^4} \left[ \frac{1}{p'^2(p^2 - m_b^2)} - \frac{1}{p'^2p^2} - \frac{m_b^2}{p'^2p^4} \right], \quad (\text{A9})$$

$$d_6^{(3)A_2} = 0, \quad (\text{A10})$$

$$d_3^A = 0, \quad (\text{A11})$$

$$d_5^A = \frac{m_u}{6p'^4(p^2 - m_b^2)^2} - \frac{m_d}{2p'^2(p^2 - m_b^2)^3}, \quad (\text{A12})$$

$$d_6^{(1)A} = -\frac{1}{81} \left[ \frac{2}{p'^2(p^2 - m_b^2)^3} - \frac{3}{p'^4(p^2 - m_b^2)^2} \right], \quad (\text{A13})$$

$$d_6^{(2)A} = \frac{2}{9m_b^4} \left[ \frac{1}{p'^2(p^2 - m_b^2)} - \frac{1}{p'^2p^2} - \frac{m_b^2}{p'^2p^4} \right], \quad (\text{A14})$$

$$d_6^{(3)A} = 0, \quad (\text{A15})$$

$$d_3^V = -\frac{m_d}{p'^2(p^2 - m_b^2)^2}, \quad (\text{A16})$$

$$d_5^V = \frac{m_u}{3p'^4(p^2 - m_b^2)^2} - \frac{m_d}{3p'^2(p^2 - m_b^2)^3} - \frac{m_d m_b^2}{2p'^2(p^2 - m_b^2)^4} - \frac{m_d(m_b^2 - q^2)}{6p'^4(p^2 - m_b^2)^3}, \quad (\text{A17})$$

$$d_6^{(1)V} = \frac{1}{81} \left[ \frac{4}{p'^2(p^2 - m_b^2)^3} - \frac{1}{p'^4(p^2 - m_b^2)^2} - \frac{6m_b^2}{p'^2(p^2 - m_b^2)^4} - \frac{2(m_b^2 - q^2)}{p'^4(p^2 - m_b^2)^3} \right], \quad (\text{A18})$$

$$d_6^{(2)V} = \frac{4}{9m_b^4} \left[ \frac{1}{p'^2(p^2 - m_b^2)} - \frac{1}{p'^2p^2} - \frac{m_b^2}{p'^2p^4} \right], \quad (\text{A19})$$

$$d_6^{(3)V} = 0. \quad (\text{A20})$$

## REFERENCES

- [1] P. Ball, V. M. Braun, and H. G. Dosch, Phys. Rev. D**44**, 3567 (1991); P. Ball, *ibid*, **48**, 3190 (1993).
- [2] V. M. Belyaev, A. Khodjamiryan, and R. Ruckl, Z. Phys. C**60**, 349 (1993).
- [3] A. Ali, V. M. Braun, and H. Simma, Z. Phys. C**63**, 437 (1993).
- [4] J. M. Flynn et al. (UKQCD coll.), Nucl. Phys. B**461**, 327 (1996); *ibid*, B**476**, 313 (1996).
- [5] J.G. Körner and G. A. Schuler, Z. Phys. C**46**, 93 (1990).
- [6] M. Wirbel, B. Stech, and M. Bauer, Z. Phys. C**29**, 637 (1985).
- [7] N. Isgur, D. Scora, B. Grinstein, and M. Wise, Phys. Rev. D**39**, 799 (1989).
- [8] D. Scora and N. Isgur, Phys. Rev. D**52**, 2783 (1995).
- [9] H.-Y. Cheng, C.-Y. Cheung, and C.-W. Hwang, Phys. Rev. D**55**, 1559 (1997).
- [10] K.-C. Yang and W-Y. P. Hwang, Z. Phys. C**73**, 275 (1997).
- [11] P. Ball and V. M. Braun, Phys. Rev. D**55**, 5561 (1997).
- [12] H.-n. Li and H.-L. Yu, Phys. Rev. Lett. **74**, 4388 (1995); H.-n. Li and H.-L. Yu, Phys. Lett. B**353**, 301 (1995).
- [13] A. V. Radyushkin and R. Ruskov, Nucl. Phys. B**481**, 625 (1996).
- [14] A. V. Smilga and M. A. Shifman, Yad. Fiz. **37**, 1613 (1983) [ Sov. J. Nucl. Phys. **37**, 958 (1983)].
- [15] K.-C. Yang, W-Y. P. Hwang, E. M. Henley, and L. S. Kisslinger, Phys. Rev. D**47**, 3001 (1993).
- [16] R. E. Cutkosky, J. Math. Phys. **1**, 429 (1960).

- [17] One should note that not all tensor structures are independent. In the case of deriving the form factor  $g$ , we choose  $S_{\alpha\mu\nu}$ ,  $S'_{\alpha\mu\nu}$ ,  $p_\mu T_{\nu\alpha} - p_\alpha T_{\mu\nu}$ ,  $p'_\mu T_{\nu\alpha} - p'_\alpha T_{\mu\nu}$ ,  $p_\nu T_{\alpha\mu}$ , and  $p'_\nu T_{\alpha\mu}$  as independent structures with  $T_{\alpha\mu} = \epsilon_{\alpha\mu\beta\rho} p'^\beta p^\rho$ ,  $S_{\alpha\mu\nu} = \epsilon_{\alpha\mu\nu\beta} p^\beta$ , and  $S'_{\alpha\mu\nu} = \epsilon_{\alpha\mu\nu\beta} p'^\beta$ . See also Ref. [10].
- [18] H. Jung and L. S. Kisslinger, Nucl. Phys. **A586**, 682 (1995).
- [19] B. L. Ioffe and A. V. Smilga, Phys. Lett. **B114**, 353 (1982); B. L. Ioffe and A. V. Smilga, Nucl. Phys. **B216**, 373 (1983).
- [20] M. Neubert, Phys. Rev. **D45**, 2451 (1991).
- [21] M. A. Shifman, A. I. Vainshtein, and V. I. Zakharov, Nucl. Phys. **B147**, 385, 448 (1979); L. J. Reinders, H. Rubinstein, and S. Yazaki, Phys. Rep. **127**, 1 (1985).
- [22] M. B. Voloshin and M. A. Shifman, Yad. Fiz. **45**, 463 (1987)[Sov. J. Nucl. Phys. **45**, 292 (1987)].
- [23] H. D. Politzer and M. B. Wise, Phys. Lett. **B206**, 681 (1988); ibid, **208**, 504 (1988).
- [24] N. Isgur and M. B. Wise, Phys. Lett. **B232**, 113 (1989); **237**, 527 (1990).
- [25] J. Govaerts, et al., Nucl. Phys. **B283**, 706 (1987).
- [26] S. J. Brodsky and G. P. Lepage, Phys. Rev. **D22**, 2157 (1980).
- [27] N. Isgur and M. B. Wise, Phys. Rev. **D42**, 2388 (1990).
- [28] M. Artuso, HEPSY 96-2, hep-ex/9610009.
- [29] J. P. Alexander et al. (CLEO Collaboration), Phys. Rev. Lett. **77**, 5000 (1996).
- [30] Particle Data Group, Phys. Rev. **D54**, 1 (1996).
- [31] K.-C. Yang, in preparation.

TABLES

TABLE I. Estimates of the  $\rho$  and  $B$  meson masses from Eqs.(39-42).

	$m_\rho$ (GeV)	$m_B$ (GeV)
Eq. (39)	0.722~ 0.806	5.15 ~ 5.28
Eq. (40)	0.820~ 0.844	4.99 ~ 5.02
Eq. (41)	0.830~ 0.852	4.92 ~ 4.95
Eq. (42)	0.764~ 0.803	4.98 ~ 5.01
Average	0.787±0.064	5.10±0.19

TABLE II. Estimates of various weak semileptonic form factors for  $D \rightarrow \rho, K^*$ .

	$A_1(0)$	$A_2(0)$	$A(0)$	$V(0)$
$D^0 \rightarrow \rho^-$	0.43±0.04	0.57±0.08	0.30±0.07	0.98±0.11
$D^0 \rightarrow K^{*-}$	0.61±0.04	0.67±0.08	0.22±0.03	1.10±0.10

### Figure Captions

Fig. 1. Diagrams for the propagator of Eq. (4). The heavy quark propagator is represented by the heavy line.

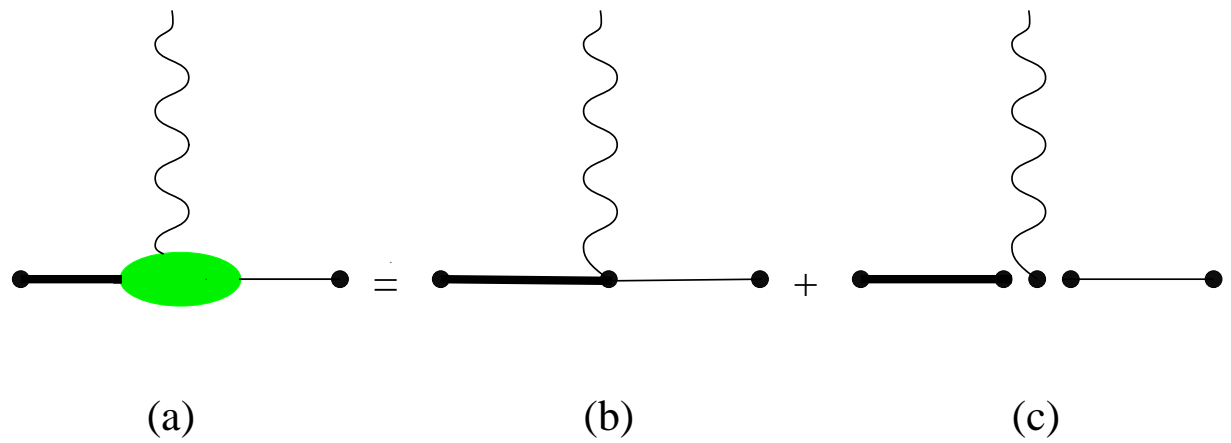
Fig. 2. Diagrams for the correlation function of Eq. (20). The heavy quark propagator is represented by the heavy line.

Fig. 3. The  $\rho$  mass and  $B$  mass, extracted from Eq. (39), plotted as a function of the square of the Borel masses  $M^2$  and  $M'^2$ .

Fig. 4. The  $\rho$  mass as a function of the square of the Borel masses  $M^2$  and  $M'^2$ . In Fig. 4(a) the  $\rho$  mass is extracted from Eq. (48), the  $A_1$  sum rule of [1]. In Fig. 4(b) the  $\rho$  mass is extracted from Eq. (49), the  $A_2$  sum rule of [11].

Fig. 5. The  $A_1(0)$ ,  $A_2(0)$ ,  $A(0)$ , and  $V(0)$  form factors plotted as a function of the square of the Borel masses  $M^2$  and  $M'^2$ .

Fig. 6. (a) The lepton-pair invariant mass spectra  $d\Gamma/dq^2$  plotted as a function of  $q^2$ . The solid curve is  $d\Gamma/dq^2$ . The long-dashed curve stands for  $d\Gamma_L/dq^2$ , the portion of the rate with a longitudinal polarized  $\rho$  in the final state. The short-dashed curve stands for  $d\Gamma_-/dq^2$ , the portion of the rate with a helicity minus  $\rho$  in the final state, while the dotted curve is for  $d\Gamma_+/dq^2$ , the portion of the rate with a helicity positive  $\rho$  in the final state. (b) The electron spectra  $d\Gamma/dE_e$  of the  $\bar{B} \rightarrow \rho^+ \ell^- \bar{\nu}_\ell$  together with  $d\Gamma_L/dE_e$ ,  $d\Gamma_+/dE_e$ , and  $d\Gamma_-/dE_e$ . The solid curve, the long-dashed curve, the short-dashed curve, and the dotted curve are for  $d\Gamma/dE_e$ ,  $d\Gamma_L/dE_e$ ,  $d\Gamma_-/dE_e$ , and  $d\Gamma_+/dE_e$ , respectively.



(a)

(b)

(c)

Fig. 1

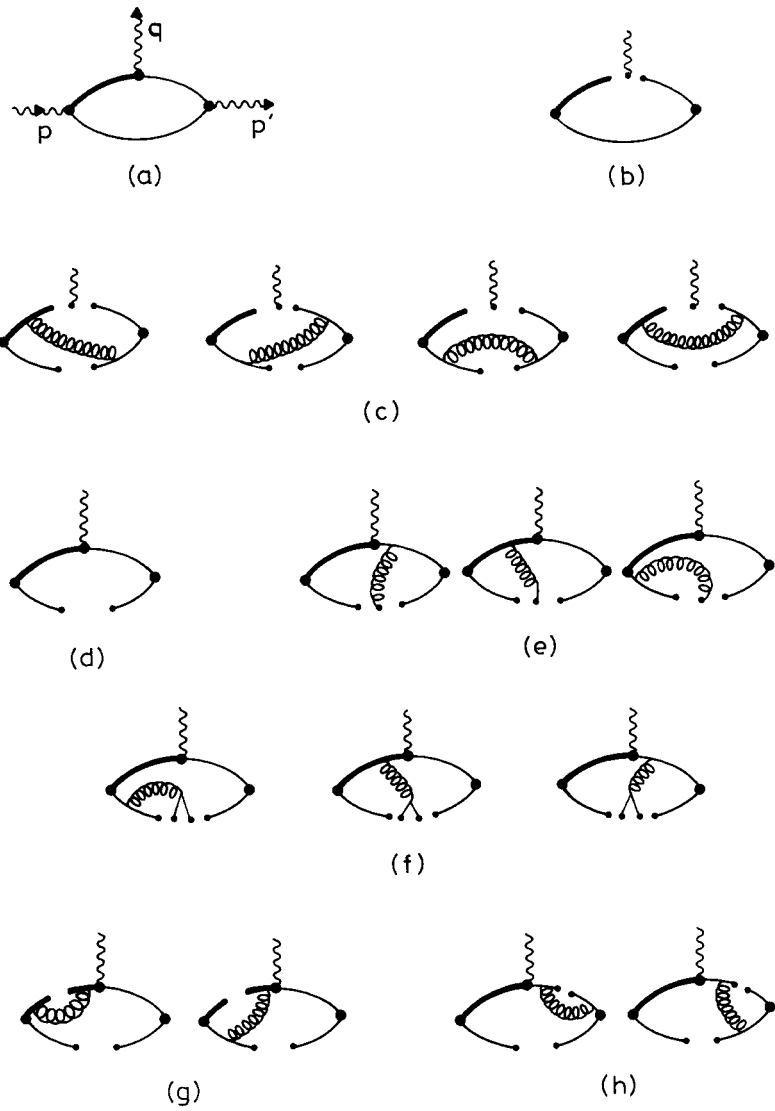


Fig. 2

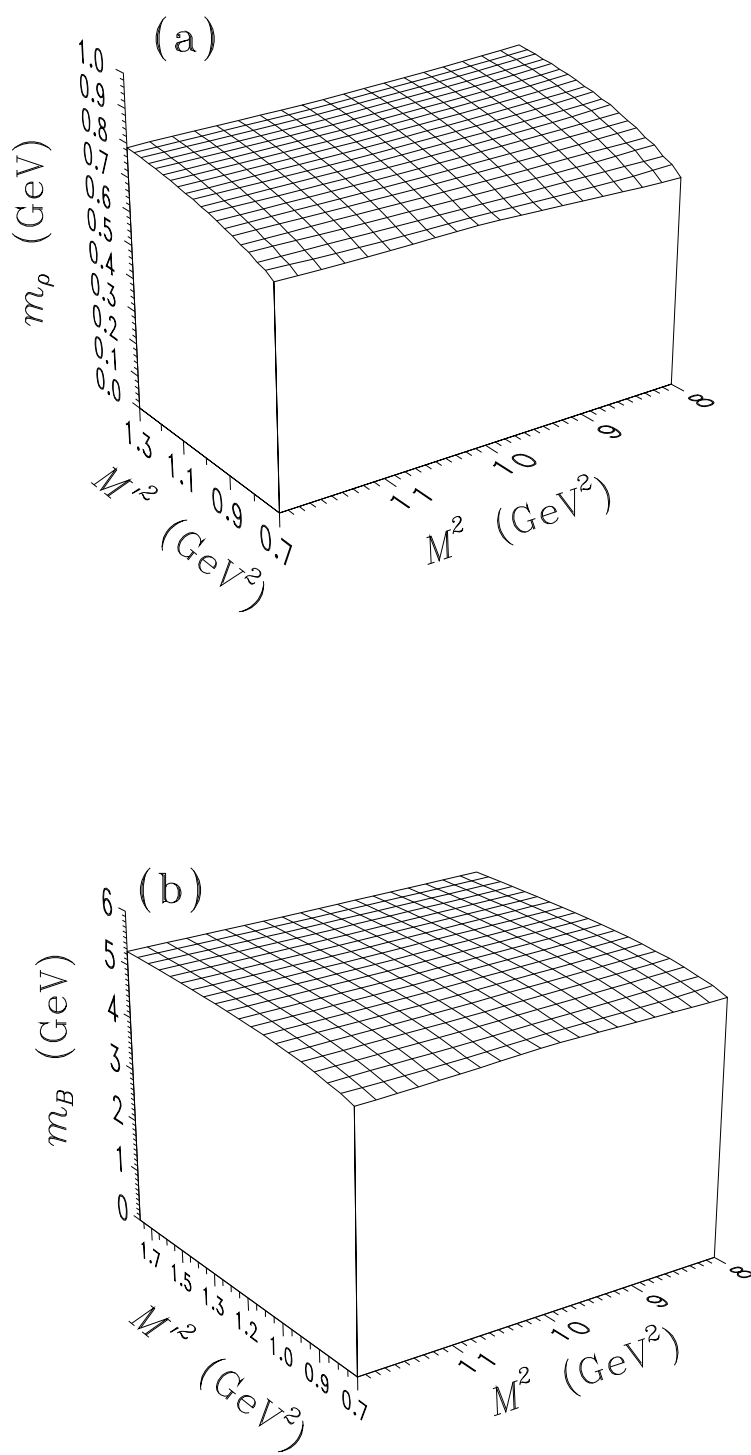


Fig. 3

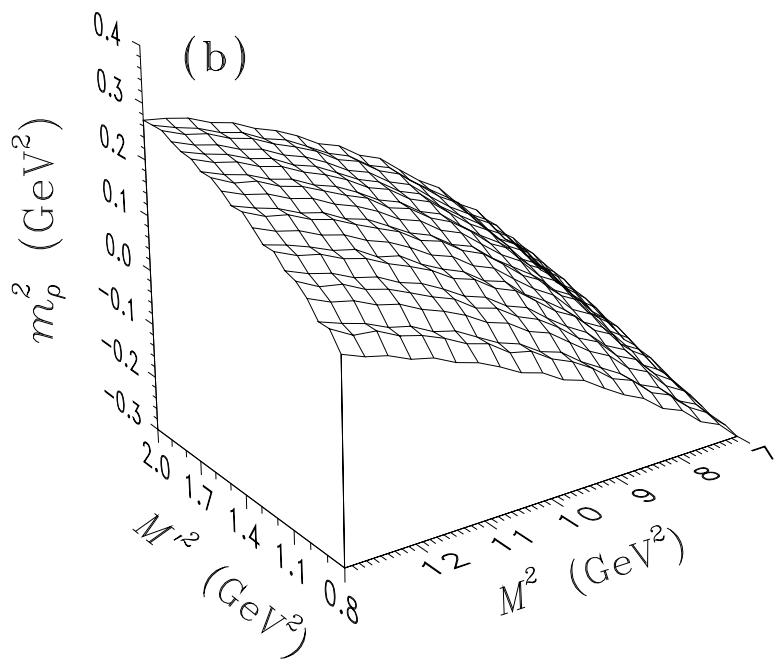
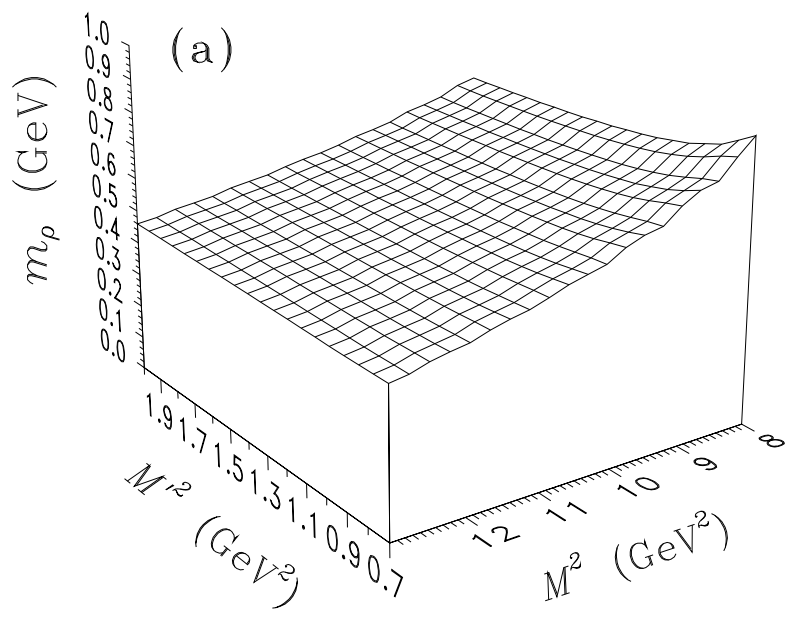


Fig. 4



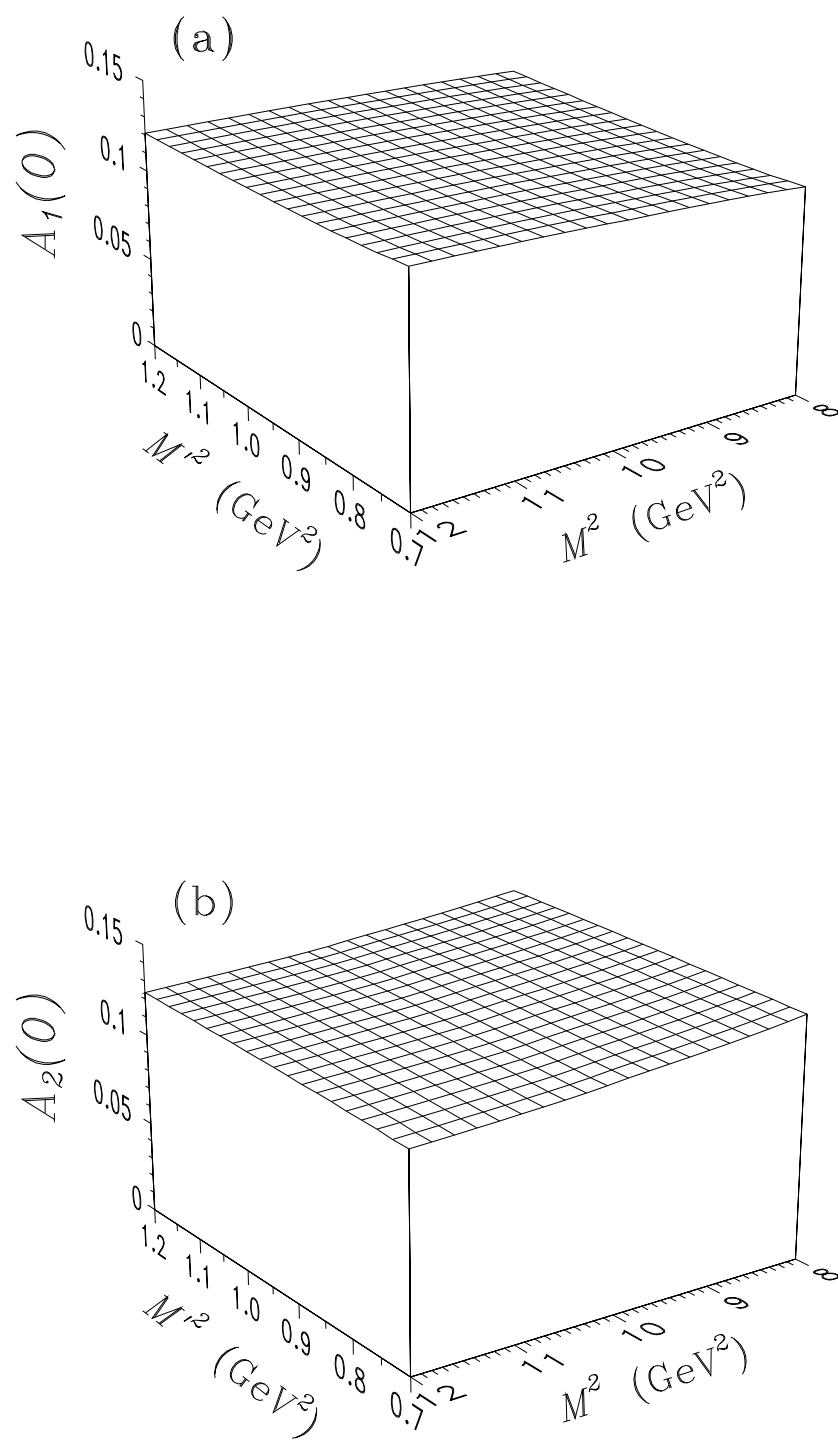


Fig. 5.1



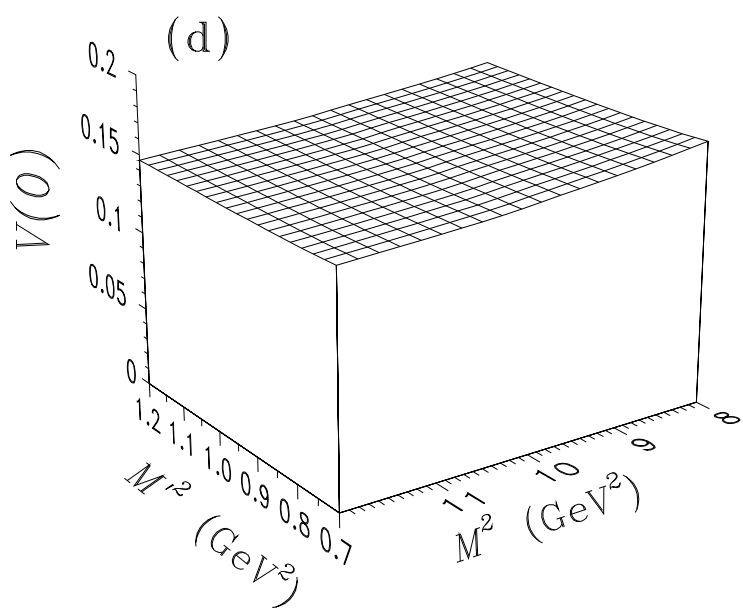
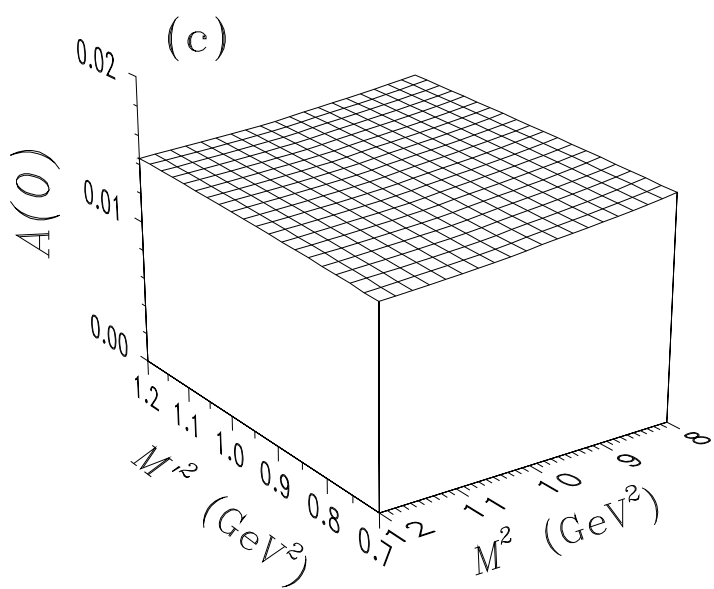


Fig. 5.2

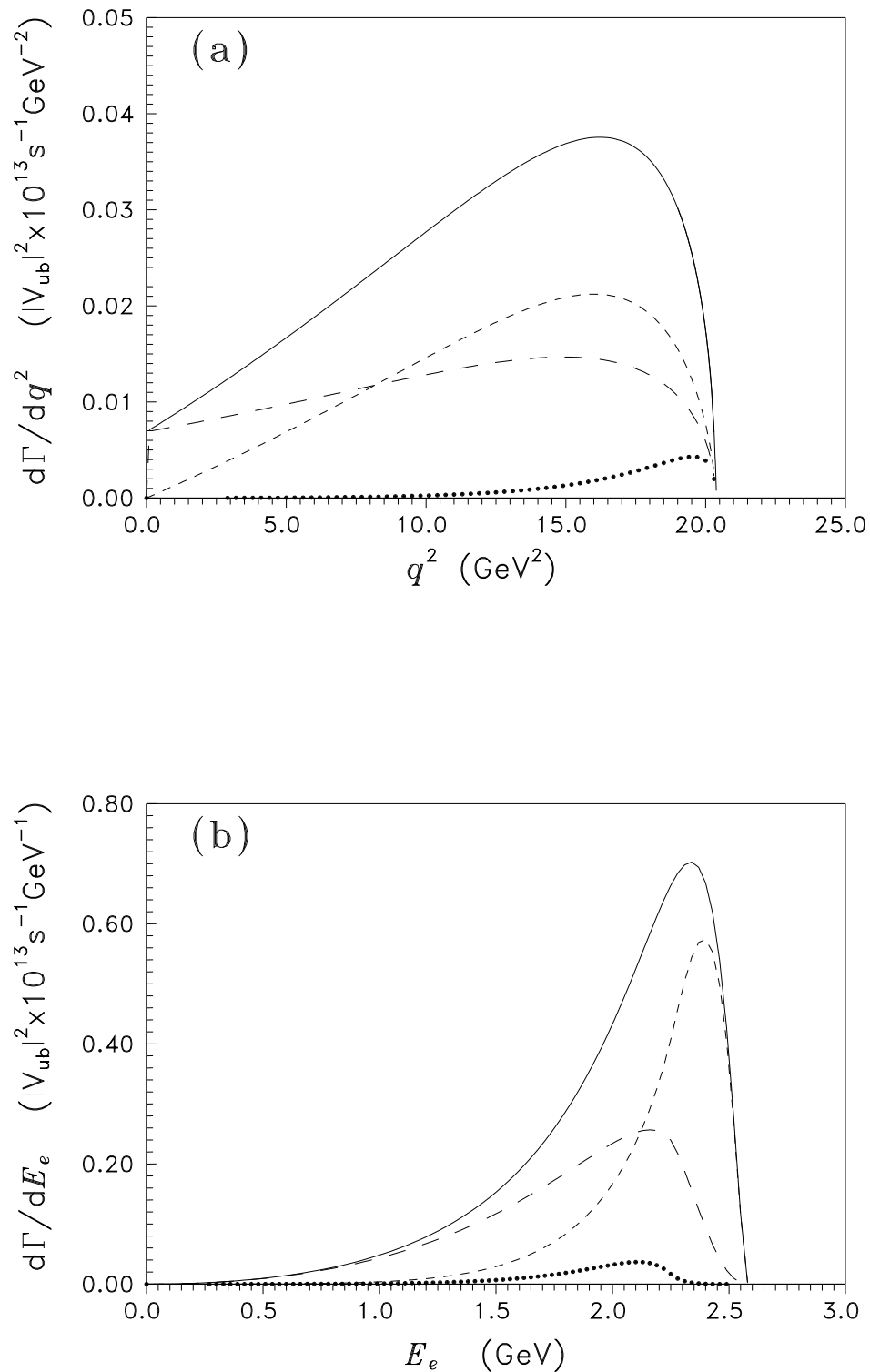


Fig. 6